

Corrosion Protection of Copper Current Collector Of Lithium-Ion Batteries by Doped Polypyrrole Coatings

Xueao Jiang^{1,2}, Jian Chen^{1,2,*}, Yang Yang^{1,2}, Yunlei Lv^{1,2}, Yanjie Ren^{1,2,*}, Wei Li^{1,2}, Cong Li^{1,2}

¹ School of Energy and Power Engineering, Changsha University of Science & Technology, Changsha, Hunan 410014, China

² Key Laboratory of Energy Efficiency and Clean Utilization, Education Department of Hunan Province, Changsha University of Science & Technology, Changsha, Hunan 410014, China

*E-mail: chenjian_513@126.com; yjren1008@163.com

Received: 31 October 2019 / Accepted: 18 December 2019 / Published: 10 February 2020

The current collector is an important multi-functional component of lithium-ion batteries. However, the degradation of current collectors in organic electrolytes influences the capacity, coulomb efficiency and even service life of the batteries. Thus, it is essential to develop a conductive and protective coating for current collectors. In this paper, polypyrrole (PPy) coatings doped with oxalic acid were electrodeposited by cyclic voltammetry technique to enhance the corrosion resistance of a copper current collector. The electrochemical degradation of the polypyrrole-coated copper was investigated by electrochemical impedance spectroscopy (EIS) at room temperature in an organic electrolyte of lithium-ion batteries. After exposure to the electrolyte for up to 500 h, the charge transfer resistance (R_t) of the polypyrrole-coated copper was ~7 times greater than that of the bare copper, indicating that polypyrrole coatings could improve the corrosion resistance of copper current collectors.

Keywords: Lithium-ion battery; Copper current collector; Polypyrrole Coating; Corrosion resistance

1. INTRODUCTION

Lithium-ion batteries have been widely used in human daily electronic products, such as mobile phones, laptops and other portable electronic devices because of their high voltage, high energy density, safety, and low self-discharge rate [1-2]. The current collector is an important component of lithium-ion batteries, because it acts as the carrier for the electrode material and collects the current during the electrochemical reaction [3]. However, anodic and cathodic current collectors are often corroded at ambient temperature of lithium-ion batteries, which causes a reduction in the capacity, coulomb efficiency and even service life of the lithium-ion batteries [4]. Zhang et al observed that aluminium current collectors are extremely prone to local corrosion in battery electrolytes containing

LiPF₆ [5]. Hyams et al compared the corrosion resistance of aluminium current collectors in high-power lithium-ion batteries under 25 °C and 45 °C cycles and found that the percentage of pit area, number of pits, pit size distribution and pit depth all increased at 45 °C [6]. Therefore, it is essential to improve the corrosion resistance of the current collector and increase the capacity and service life of the battery [7-8]. Liu et al prepared artificial SEI films that exhibited high strength, flexibility, high conductivity and an improved protective performance by the direct contact of Cu₃N nanoparticles and styrene butadiene rubber on the surface of the current collector [9]. Kozen et al used an atomic layer deposition method to prepare a 14 nm thick aluminium oxide coating on the surface of lithium metal, and it was found that the layer was relatively stable and protected the surface of the lithium metal from air and electrolyte corrosion [10]. Copper is often used as the negative current collector in lithium-ion batteries due to its good conductivity, low cost and large-scale suitability [11-12]. However, in the working environment of the negative electrode in a lithium-ion battery, the copper current collector is easily corroded due to the decomposition product of the HF electrolyte and the residual minimal amount of water [13].

Conductive polymers, for example, polypyrrole or its derivatives, are mainly used in the fields of metal materials corrosion protection, electrochemistry and optics [14-17]. The application of polypyrrole to protect copper against corrosion has been reported by several authors. Jaouhari et al electrodeposited polypyrrole on copper in a dodecylbenzenesulfonic acid solution and found that a polypyrrole coating could provide excellent corrosion protection for copper [18]. At present, the corrosion performance of polypyrrole on a copper current collector in an organic electrolyte used in lithium-ion batteries is not available.

In this paper, a polypyrrole coating was electrodeposited on copper aiming to evaluate its potential applications as a corrosion resistant and conductive coating for the anode current collector in lithium-ion batteries [19-20].

2. EXPERIMENTAL PROCEDURES

2.1 Electrodeposition of polypyrrole coatings

Commercial T1 copper (99.95 % purity, with dimensions of 1 cm × 1 cm × 1.1 cm) was chosen as the base material. Samples with an exposed area of 1.1 cm² were coated with epoxy resin, then were polished with 600-grit emery paper, cleaned in distilled water and degreased in acetone. The polypyrrole coatings were synthesized in a solution containing 0.4 mol/L pyrrole and 0.3 mol/L oxalic acid by cyclic voltammetry (CV) technique with a potential sweep between -0.2 V (SCE) to 1.05 V (SCE) for 10 times while the scanning rate was set to 30 mV/s.

The polypyrrole film was electrodeposited using an electrochemical workstation (Zahner Zennium) at room temperature. A conventional three-electrode system was chosen for this electrochemical measurement with a copper sheet as the counter electrode, a saturated calomel electrode (SCE) as the reference electrode, the bare and polypyrrole-coated copper samples as the working electrode.

2.2 Electrochemical Measurements

The electrolyte used in lithium-ion batteries contains 1 M LiPF_6 in a mixture of ethylene carbonate (EC), methyl ethyl carbonate (EMC) and dimethyl carbonate (DMC) (1:1:1, V/V/V). The subsequent electrochemical measurements were also performed with a conventional three-electrode system, with a copper sheet as the counter electrode and a silver wire as the reference electrode. Electrochemical impedance measurements were carried out between 10^{-2} Hz and 10^{+5} Hz at open-circuit potential. The amplitude of the input sine-wave voltage was 10 mV.

3. RESULTS AND DISCUSSION

3.1 Preparation of polypyrrole coatings

Figure 1 shows the cyclic voltammograms for the synthesis of the polypyrrole in a solution containing pyrrole and oxalic acid. An oxidation peak at 0.1 V is observed during the first cycle, and then, it disappears in the subsequent cycles. This oxidation peak is related to the anodic oxidation of the copper. It has been demonstrated that dissolved Cu^{2+} species promote the polymer yield during the synthesis of conducting polymers and improve the stability of polypyrrole layers on copper electrodes [21]. The onset of electropolymerization is observed at approximately 0.75 V (SCE), and this value shifts negatively during the following positive cycles due to the self-catalyst behaviour from the growth of the polypyrrole.

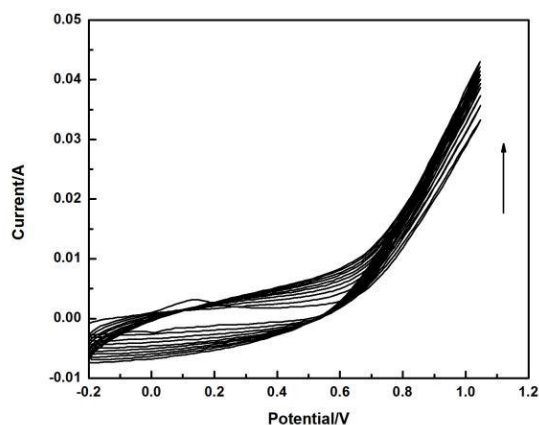


Figure 1. Cycle voltammetry curves for the synthesis of the PPy coating on copper

3.2. Characterization of polypyrrole coatings

Figure 2 shows the surface morphology of the bare copper and as-deposited polypyrrole coating before and after immersion in the electrolyte used in lithium-ion batteries for 500 h. The surface of the as-deposited polypyrrole coating is homogeneous with a cauliflower-like structure. The

polypyrrole adheres strongly to the electrode and is difficult to peel off. After immersion for 500 h in the electrolyte, obvious holes are observed on the copper surface. However, no corrosion products are observed for the polypyrrole coating for the entire immersion time.

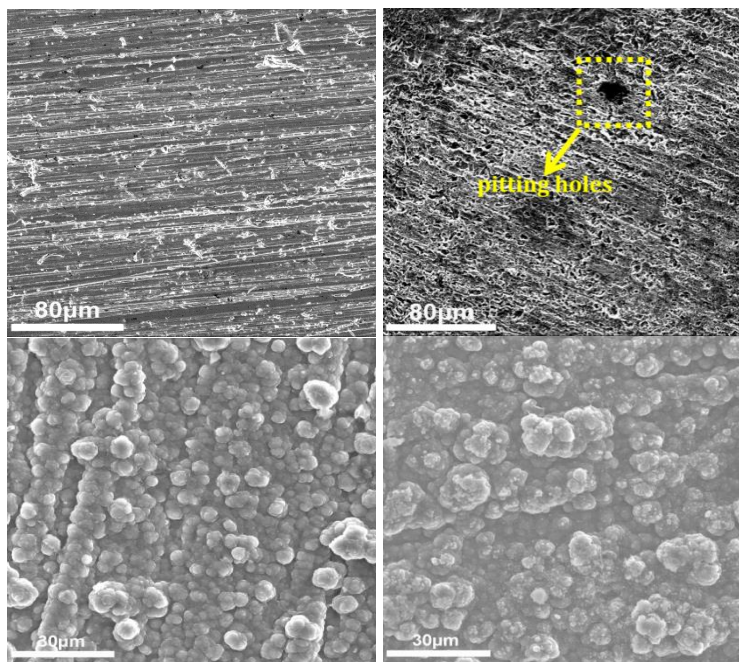


Figure 2. Surface morphology of the bare copper and the as-deposited PPy coating before and after immersion in the electrolyte for 500 h

3.3. Electrochemical polarization measurements

Figure 3 shows the potentiodynamic polarization curves for the bare and polypyrrole-coated copper after immersion in the electrolyte at room temperature for 3 h. Based on the Tafel equations, the corrosion potential (E_{corr}) and the corrosion current density (I_{corr}) of the bare copper are -0.147 V and $7.244 \mu\text{A}\cdot\text{cm}^{-2}$, respectively, while those for polypyrrole-coated copper are 0.123 V and $5.263 \mu\text{A}\cdot\text{cm}^{-2}$, respectively. That is, the polypyrrole coating causes the positive shift in E_{corr} by more than 0.25 V in comparison to that of the bare copper, indicating an increased redox potential. Generally, the protectiveness of conductive polymers stems from their electro-catalytic oxidation effects for the metals due to their high electrochemical activity [22]. Therefore, it could be observed that the corrosion current of the polypyrrole coating is close to that for the bare copper.

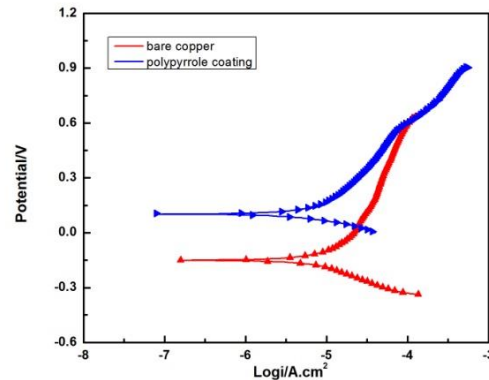


Figure 3. Potentiodynamic curves of bare and PPy-coated copper in the electrolyte after immersion in the electrolyte for 3 h (scanning rate: 1 mV/s)

3.4 Open circuit potential versus Time curves

Figure 4 presents the open-circuit potential (E_{ocp}) versus time curves for the bare and polypyrrole-coated copper in the organic electrolyte used in lithium-ion batteries. For the bare copper, there is a sharp decrease from -0.314 V (SCE) to -0.586 V (SCE) after immersion for 2 h and then, the value remains nearly constant with the immersion time of up to 500 h. For polypyrrole coated copper, the initial value of E_{ocp} decreases from -0.1 V (SCE) to -0.15 V (SCE) and then increases for the total immersion time with some fluctuations. The decrease in E_{ocp} for the polypyrrole coatings at the initial stage is related to the penetration of the electrolyte into the polymer. The subsequent passivation of the film/substrate alloy interface contributes to an increase in the E_{ocp} .

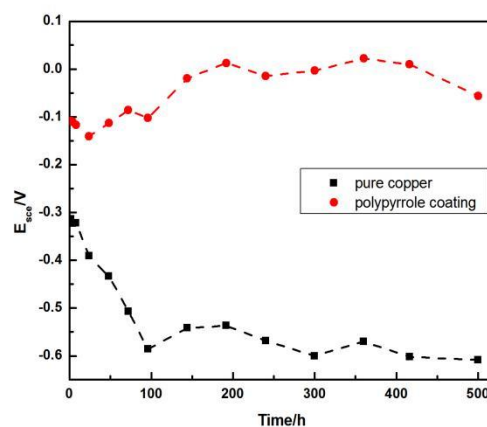


Figure 4. Open circuit potential-time curve of bare copper and PPy-coated copper immersed in the electrolyte of lithium-ions batteries

3.5 Electrochemical impedance spectroscopy

Figure 5 shows the typical Nyquist and Bode plots for copper immersed in the electrolyte for different lengths of time. The Nyquist plots include two distinct depressed loops. The capacitive loops

at high frequencies indicate the information about the corrosion product film on the surface of the copper, and the capacitive loops at low frequencies indicate information about the electrochemical reaction at the substrate/solution interface. As the immersion time increases, the capacitive loops contract significantly, indicating an increasing copper corrosion rate. Furthermore, the depression in the phase angle in the low and middle frequency regions after immersion for 24 h also indicated a gradual degradation of the dense corrosion product.

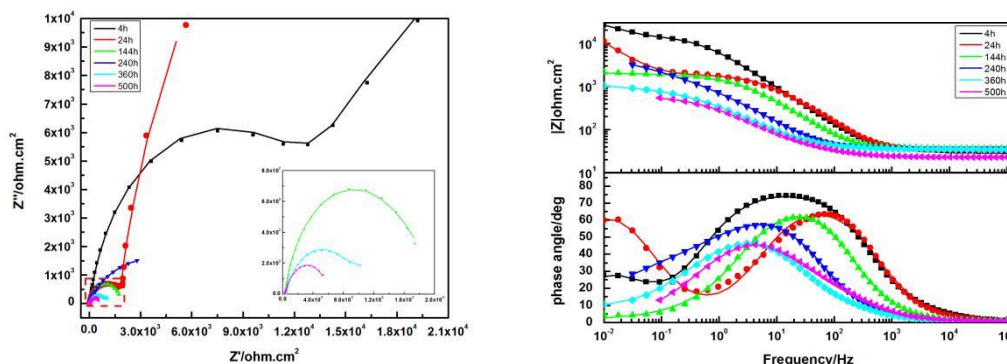


Figure 5. Nyquist and Bode plots of copper foil corroded in the electrolyte of lithium-ion batteries with prolonged immersion time. Symbols: experimental data; line: fitted data

Figure 6 shows the typical Nyquist curves and Bode plots of the polypyrrole-coated copper exposed to the electrolyte for different exposure times. It contains two time constants for the total immersion time. The high-frequency section reflects the responses from the films and the low-frequency part reflects the responses from the electrochemical reaction occurring at the film/substrate alloy interface. The capacitive loop shrinks as the immersion time increased, indicating that the electrolyte penetrates the polymer. The decrease in the corrosion resistance of polypyrrole is also supported by the depression in the phase angle in the high frequency domain.

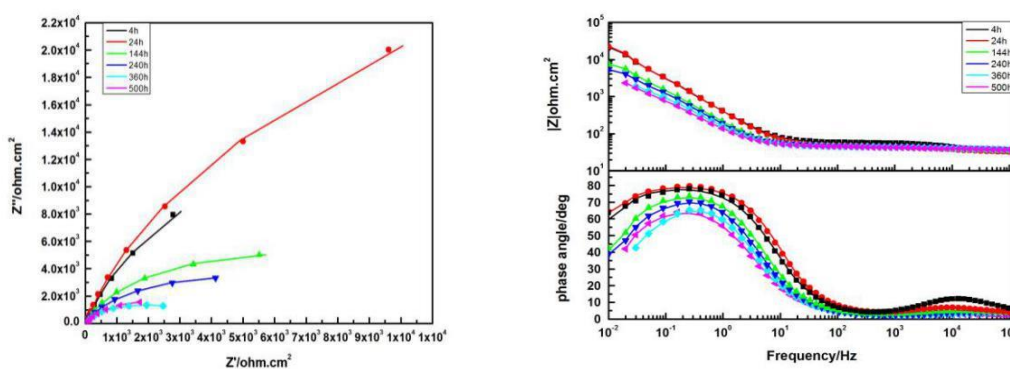


Figure 6. Nyquist and Bode diagrams of the PPy coating in the electrolyte. Symbols: experimental data; line: fitted data

An equivalent circuit was used to fit the electrochemical impedance spectrum from the corrosion of the bare and polypyrrole-coated copper in the electrolyte(as shown in Figure 7). In the equivalent circuit, R_s is the solution resistance of the electrolyte, C_f and R_f represent the capacitance

and resistance of the corrosion product layer or polypyrrole coatings on the copper, R_t and C_{dl} represent the charge transfer resistance and a double layer capacitance, respectively. In this equivalent circuit, considering the dispersion effect, a constant phase element, CPE (Q), is used instead of the pure capacitor C to determine the surface reaction, surface heterogeneity, roughness, electrode porosity and voltage-current distribution which are associated with electrode geometry [7]. Figure 8 shows a representative error plot for the polypyrrole coating. The maximum error is less than 1.4 % in $|z|$ and less than 1 % for the angles of all fitted impedance spectra, so it can be considered that the equivalent circuit was suitable for the bare and polypyrrole-coated copper samples.

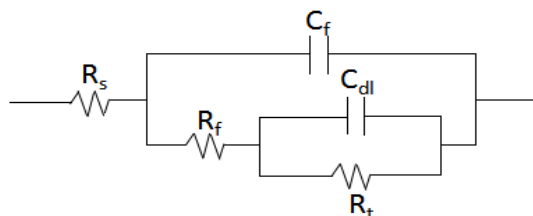


Figure 7. Equivalent circuit for the fitting of impedance spectroscopy

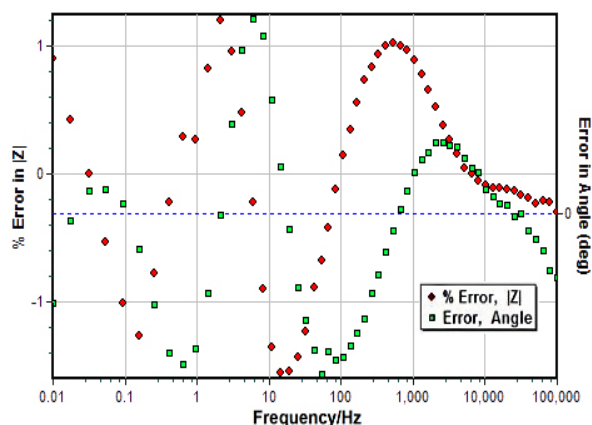


Figure 8. Error plots for calculated values of $|z|$ and the phase angle of PPy coatings immersed for 100 h in the electrolyte

The electrochemical parameters obtained from the fitting of the impedance spectra are listed in Tables 1 and 2. R_t is usually used to evaluate the resistance of the electron transfer across a metal surface, and it is inversely proportional to the corrosion rate of the metal [23]. According to Table 1, R_t decreases with increasing soaking time, suggesting that the resistance of the electrochemical reaction process is reduced. The parameter n_{dl} is related to the surface roughness of the electrode, and the value of n_{dl} decreases from 0.8978 to 0.6648, indicating an inhomogeneous corrosion of the copper.

For the polypyrrole coating, R_f is the sum of the electronic resistance R_e which indicates the migration of the electrons in the conductive polypyrrole chains, and the ionic resistance R_i of the electrolyte within the pores of polypyrrole. The R_f of the coating decreases from $28.30 \Omega \cdot \text{cm}^2$ to $16.41 \Omega \cdot \text{cm}^2$ after immersion in the electrolyte for 24 h and then remains stable for the total 500 h immersion in the electrolyte. The decrease in the initial stage is related to the penetration of the organic electrolyte

into the bulk of the polypyrrole coating. Then, R_f remains at approximately $16 \Omega \cdot \text{cm}^2$ which is significantly lower than that for the corrosion production film formed on the bare copper. That is, the conductive polypyrrole decreases the electric resistance of the copper current collector corroded in the organic electrolyte [24]. The R_t values for the polypyrrole coating increase from $5.999\text{E}4 \Omega \cdot \text{cm}^2$ to $8.372\text{E}4 \Omega \cdot \text{cm}^2$ in the early stage, decrease and fluctuate at prolonged immersion times. After immersion for 500 h, the R_t value is ~ 7 times greater than that of the bare copper, indicating that polypyrrole coating could provide protection for the copper.

Table 1. Fitting results of impedance spectra for bare copper immersed in the electrolyte of lithium-ions batteries

Time (h)	R_s ($\Omega \cdot \text{cm}^2$)	Y_f ($\text{S}^{-\alpha} \Omega^{-1} \text{cm}^{-2}$)	n_f	R_f ($\Omega \cdot \text{cm}^2$)	Y_{dl} ($\text{S}^{-\alpha} \Omega^{-1} \text{cm}^{-2}$)	n_{dl}	R_t ($\Omega \cdot \text{cm}^2$)
4	32.81	2.794E-5	0.8590	1.825E4	1.139E-3	0.8978	5.214E4
24	31.73	2.757E-5	0.8785	1.439E4	4.783E-4	0.8341	3.131E4
144	36.27	4.824E-5	0.8969	7.965E3	1.519E-4	0.5146	1.189E4
240	35.65	2.156E-4	0.8333	5.569E2	4.674E-4	0.5600	1.252E4
360	34.73	7.101E-4	0.7121	8.927E2	2.036E-4	0.6371	3.812E2
500	22.84	2.413E-4	0.8167	0.452E2	5.692E-4	0.6648	5.901E2

Table 2. Fitting results of impedance spectra for PPy coated copper immersed in the electrolyte of lithium-ions batteries

Time (h)	R_s ($\Omega \cdot \text{cm}^2$)	Y_f ($\text{S}^{-\alpha} \Omega^{-1} \text{cm}^{-2}$)	n_f	R_f ($\Omega \cdot \text{cm}^2$)	Y_{dl} ($\text{S}^{-\alpha} \Omega^{-1} \text{cm}^{-2}$)	n_{dl}	R_t ($\Omega \cdot \text{cm}^2$)
4	29.84	1.564E-5	0.7086	28.30	4.740E-4	0.9051	5.999E4
24	31.00	5.099E-5	0.6700	16.41	4.303E-4	0.9295	8.372E4
144	32.91	9.806E-5	0.6150	13.23	8.996E-4	0.9048	1.289E4
240	43.63	1.383E-5	0.8576	17.16	1.355E-3	0.7598	1.775E4
360	33.11	1.733E-5	0.5199	12.12	1.334E-3	0.8751	3.683E3
500	36.36	2.331E-4	0.6211	8.929	1.611E-3	0.8489	4.518E3

In the organic electrolyte used in lithium-ion batteries, the residual minimal amounts of water could oxidize the copper and form CuO_x . Electrochemical corrosion usually occurs at the defects present in oxide films and subsequently destroys the films. The HF decomposition product of the electrolyte adsorbs on the oxide film and destroys the CuO_x film with the production of H_2O and CuF_2 [25]. The residual water in the attacked zone causes local electrochemical corrosion as a self-catalyst and promotes the propagation of pits [26]. Thus, obvious holes are observed on the surface of the copper after immersion for 500 h in the organic electrolyte, as shown in Figure 2.

The ability of conductive polymers to protect metals stems from passivation effects [27]. For polypyrrole films doped with oxalic anions, the passivation effect is available during electropolymerization processes due to the formation of insoluble compounds on the surface of copper. It is known that an oxalate anion easily forms a stable complex with a copper cation, in particular, the oxalate anion (O_x^{2-}) and Cu^{2+} can form insoluble copper oxalates complexes $\text{Cu}(\text{O}_x)$ and $[\text{Cu}(\text{O}_x)_2]^{2-}$ by

stoichiometric ratios of 1:1 and 1:2, respectively [28]. These conditions cause electrode passivation by forming a thin insoluble copper oxalate layer which protects metals from dissolution without affecting the electropolymerization process [29]. As the corrosive species in the organic electrolyte travels through the defects of conductive polymers and into the interface of coating/copper and attack the substrate, the polypyrrole polymer is apt to oxidize the copper and polypyrrole reduces to maintain the copper in passivated state. Thus, the self-healing effects could be observed from the fluctuations in the E_{ocp} , as shown in Figure 3. The obvious increase in R_t upon immersion in the electrolyte for 24 h also indicates that the electrolyte penetrated the coating/substrate interface through the microscopic pores in the coating and passivation of the underlying copper. Moreover, the products of the concomitant redox reaction with polypyrrole salt and the oxalate anions are released, which weakens of the catalytic oxidation of the copper matrix, R_t values decrease to $4518 \Omega \cdot \text{cm}^2$ after immersion for 500 h consequently. Nonetheless, the value of R_t is still greater than that of the bare copper. In addition, no delamination or blistering of the polypyrrole coatings are observed after being immersed for 500 h immersion in the organic solution (as shown in Figure 1d), which is related to the shift in location of the cathodic reaction from metal substrate to the interface of polymer/electrolyte, as reported in Ref [30]. According to the above arguments, the as-deposited polypyrrole coatings improve the corrosion resistance of copper in the organic electrolyte of lithium-ion batteries.

4. CONCLUSIONS

In this study, a polypyrrole coating doped with oxalic acid was synthesized by cyclic voltammetry technique on a copper current collector that is used for lithium-ion batteries. Electrochemical methods were used to evaluate the corrosion performance of polypyrrole coatings in the organic electrolyte containing LiPF_6 . The E_{ocp} versus time curves show that the polypyrrole coating maintained a high open circuit potential after immersion in an electrolyte used for lithium-ion batteries for 500 h, indicating that the polymer coating improved the corrosion resistance of the copper. After soaking for 500 h, the charge transfer resistance (R_t) of the polypyrrole-coated copper was ~ 7 times higher than that of the bare copper. The polypyrrole coatings improved the corrosion resistance of the copper current collector in the organic electrolyte.

ACKNOWLEDGMENTS

This work was supported by the National Natural Science Foundation of China (No.51471036 and No.51771034), and Hunan Graduate Research Innovation Project (No.CX2018B559).

References

1. L.J. Li, Q. Yao, Z.Y. Chen, L.B. Song, T. Xie, H.L. Zhu, J.F. Duan, K.L. Zhang, *J. Alloy Compd.*, 650 (2015) 684.
2. W.D. Chen, J. Liang, Z.H. Yang and G. Li, *Energy Procedia*, 158 (2019) 4363.
3. H. Nara, D. Mukoyama, R. Shimizu, T. Momma and T. Osaka, *J. Power Sources*, 409 (2019) 139.

4. N. Piao, L. Wang, T. Anwar, X.N. Feng, S. Sheng, G.Y. Tian, J.L. Wang, Y.P. Tang and X.M. He, *Corros. Sci.*, 158 (2019) 108100.
5. X.Q. Zhang, X.B. Cheng, X. Chen, C. Yan and Q. Zhang, *Adv. Funct. Mater.*, 27 (2017) 1605989.
6. T.C. Hyams, J. Go and T.M Devine, *J. Electrochem. Soc.*, 154 (2007) 390.
7. J. Shu, M. Shui, F.T. Huang, D. Xu, Y.L. Ren, L. Hou, J. Cui and J.J. Xu, *Electrochim. Acta*, 56 (2011) 3006.
8. S.W. Dai, J. Chen, Y.J. Ren, Z.M. Liu, J.L. Chen, C. Li, X.Y. Zhang, X. Zhang and T.F. Zeng, *Int. J. Electrochem. Sci.*, 12 (2017) 10589.
9. Y.Y. Liu, D.C. Lin, P.Y. Yuen, K. Liu, J. Xie, R.H. Dauskardt and Y. Cui, *Adv. Mater.*, 29 (2017) 1605531.
10. A.C. Kozen, C.F. Lin, A.J. Pearse, M.A. Schroeder, X.G. Han, L.B. Hu, S.B. Lee, G.W. Rubloff and M. Noked, *ACS Nano*, 9 (2015) 5884.
11. W. Yuan, J. Luo, Z.G. Yan, Z.H. Tan and Y. Tang, *Electrochim. Acta*, 226 (2017) 89.
12. H.C. Chu, H.Y. Tuan, *J. Power Sources*, 346 (2017) 40.
13. Q.S. Wang, L.H. Jiang, Y. Yu, J.H. Sun, *Nano Energy*, 55 (2019) 93.
14. J.F. Duan, C. Zhu, Y.H. Du, Y.L. Wu, Z.Y. Chen, L.J. Li, H.L. Zhu and Z.Y. Zhu, *J. Mater. Sci.*, 52 (2017) 10470.
15. Y.B. Lee, D.S. Lim, *Curr. Appl. Phys.*, 10 (2010) S18.
16. L. Jiang, J.A. Syed, Y.Z. Gao, Q.X. Zhang, J.F. Zhao, H.B. Lu and X.K. Meng, *Appl. Surf. Sci.*, 426 (2017) 87.
17. Z.H. Chen, W.Z. Yang, B. Xu, Y.Y. Guo, Y. Chen, X.S. Yin and Y. Liu, *Prog. Org. Coat.*, 122 (2018) 159.
18. A. El Jaouhair, A. EL Asbahani, M. Bouabdallaoui, Z. Aouzal, D. Filotas, E.A. Bazzaoui, L. Nagy, G. Nagy, M. Bazzaoui, A. Albourine and D. Hartmann, *Synth. Met.*, 226 (2017) 15.
19. D. Lepage, L. Savignac, M. Saulnier, S. Gervais and S.B. Schougaard, *Electrochem. Commun.*, 102 (2019) 1.
20. A. Nautiyal, M.Y. Qiao, J.E. Cook, X.Y. Zhang and T.S. Huang, *Appl. Surf. Sci.*, 427 (2018) 922.
21. M.I. Redondo, C.B. Breslin, *Corros. Sci.*, 49 (2007) 1765.
22. Y.J. Ren, J. Chen, C.L. Zeng, C. Li and J.J. He, *Int. J. Hydrogen. Energ.*, 41 (2016) 8542.
23. C. Shanmugham, N. Rajendran, *Prog. Org. Coat.*, 89 (2015) 42.
24. A.M. Eldesoky, M.A. Diab, A.A. Ei Bindary, A.Z. Ei Sonbati and H.A. Seyam, *J. Mater. Environ. Sci.*, 6 (2015) 2148.
25. A.S. Fouda, A.M. Eldesoky, A.Z. Ei-Sonbati and S.F. Salam, *Int. J. Electrochem. Sc.*, 9 (2014) 1867.
26. A.El Jaouhari, M.Laabd, E.A. Bazzaoui, A. Albourine, J.I. Martins, R. Wang, G. Nagy and M. Bazzaoui, *Synthetic Met.*, 209 (2015) 11.
27. P.P. Deshpande, N.G. Jadhav, V.J. Gelling, D. Sazou, *J. Coat. Technol. Res.*, 11 (2014) 473.
28. B. Duran, M.C. Turhan, G. Bereket, A.S. Sarac, *Electrochim. Acta*, 55 (2009) 104.
29. P. Herrasti, A.I. del Rio, J. Recio, *Electrochim. Acta*, 52 (2007) 6496.
30. Y.J. Ren, M.R. Anisur, W. Qiu, J.J. He, S. Al-Saadi and R.K.S. Raman, *J. Power Sources*, 362 (2017) 366.